



Design and synthesis of fluorescent 6-aryl[1,2-c]quinazolines serving as selective and sensitive ‘on-off’ chemosensor for Hg²⁺ in aqueous media

Rampal Pandey, Mahendra Yadav, Mohammad Shahid, Arvind Misra*, Daya Shankar Pandey*

Department of Chemistry, Faculty of Science, Banaras Hindu University, Varanasi 221005, U.P., India

ARTICLE INFO

Article history:

Received 11 March 2012

Revised 26 April 2012

Accepted 27 April 2012

Available online 2 May 2012

Keywords:

Synthesis

Quinazolines

Crystal structure

UV-vis

Fluorescence

Mercury selective

Quenching

ABSTRACT

Three fluorescent quinazolines thiophen-2-yl-5,6-dihydrobenzo-[4,5]imidazo[1,2-c]quinazoline (**1**), pyridin-3-yl-5,6-dihydrobenzo-[4,5]imidazo[1,2-c]quinazoline (**2**) and phenyl-5,5',6,6'-dihydrobenzo-[4,4',5,5']imidazo-[1.1',2-c,2'-c]quinazoline (**3**) have been synthesized. Structures of **1** and **3** have been authenticated crystallographically. Quinazolines **1–3** exhibit highly selective ‘on-off’ switching for Hg²⁺ ions. The fluorescence intensity displayed a linear relationship with respect to Hg²⁺ concentration (0.1–1.0 μM; R² = 0.99) with detection limit of 2.0 × 10⁻⁷ M.

© 2012 Elsevier Ltd. All rights reserved.

Development of optical methods for the selective detection of certain transition/post-transition metal ions in environment and biological systems has attracted considerable current interest.¹ In this context, numerous fluorescent sensors have been synthesized due to their high sensitivity, selectivity and possible applications in various areas.² Mercury is an important metal and its accumulation in liver, kidney and spleen leads to DNA damage, mitosis impairment and nervous system defects.³ Despite being toxic, Hg and its salts are used in a number of industrial processes and products. Therefore, extensive studies have been devoted towards designing of new fluoroionophores and the development of sophisticated techniques for the detection and removal of Hg²⁺ from living systems.⁴ Owing to its *d*¹⁰ configuration Hg²⁺ lacks optical spectroscopic signature. Thus its optical detection is achieved by monitoring changes in the UV-vis or fluorescence resulting from Hg²⁺ induced perturbations of a chromophore. Although, numerous Hg²⁺ selective and sensitive sensors have been reported,⁵ chemosensors possessing high selectivity towards Hg²⁺ against a background of competing analytes in aqueous medium are highly demanding.⁶

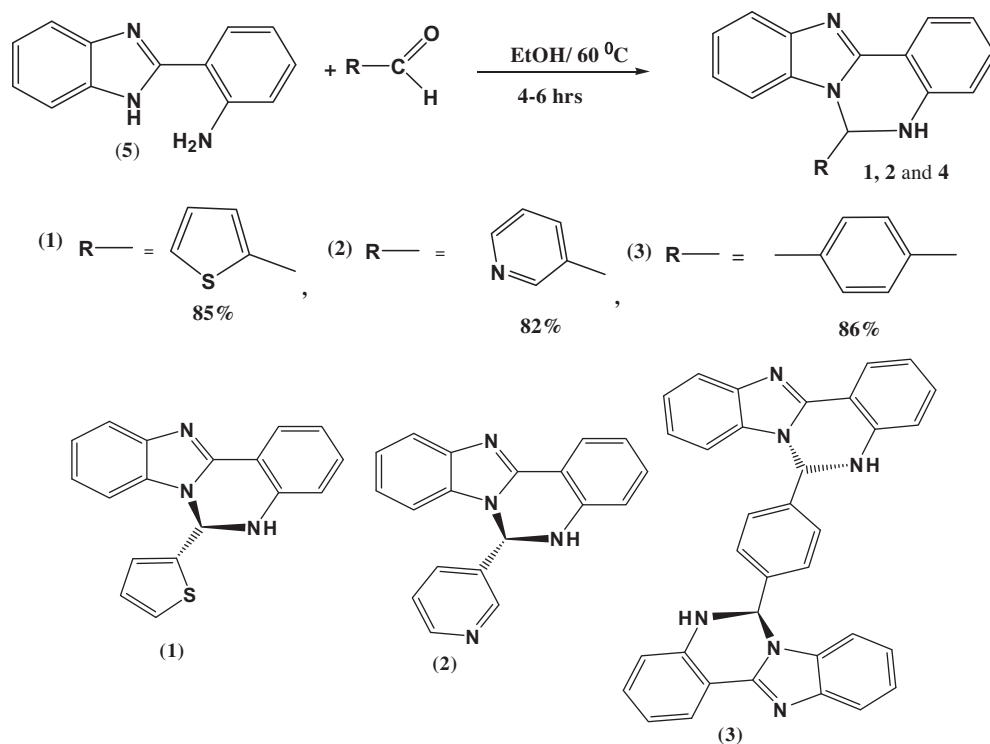
Quinazoline derivatives find widespread applications as antagonists, DNA-biosensors, epidermal growth factor receptor-tyrosine kinase (EGFR-TK) imaging, activin-like kinase (ALK5) inhibitors etc., however, their fluorescent properties have not been thoroughly explored.⁷ Although, the use of quinazoline derivatives

in the detection of metal ions is well documented, to our knowledge their application towards Hg²⁺ sensing has not been reported.⁸ The biological importance and unexploited fluorescent properties of quinazolines motivated us to develop new derivatives having a suitable recognition site for metal ions. With these points in mind three new fluorescent quinazolines viz., thiophen-2-yl-5,6-dihydrobenzo[4,5]imidazo[1,2-c]quinazoline **1**, pyridin-3-yl-5,6-dihydrobenzo[4,5]imidazo[1,2-c]quinazoline **2** and phenyl-5,5',6,6'-dihydrobenzo[4,4',5,5']imidazo[1,1',2-c,2'-c]quinazoline **3** have been designed and synthesized. With an objective of developing compounds containing different heterocyclic rings at 6-position of a quinazoline ring, **1–3** have been designed and synthesized (Scheme 1). Among these, **1** and **2** contain thiophene ‘S’ and pyridyl ‘N’ at the chelating and non-chelating sites, while **3** does not have any heteroatom at chelating position of the quinazoline nitrogen (–NH). Through this contribution we present the syntheses, characterizations and applications of **1–3** in selective detection of Hg²⁺ over a wide range of interfering cations in aqueous media.

The quinazolines **1–3** and precursor 2-(2-aminophenyl)-1-benzimidazole (**4**) were synthesized by a general procedure outlined in Scheme 1 (Figs. S1–S4, Supplementary data).⁹ Condensation of **4** with the corresponding aldehyde in ethanol afforded the aminated probes thiophen-2-yl-5,6-dihydrobenzo[4,5]-imidazo[1,2-c]quinazoline **1**, pyridin-3-yl-5,6-dihydrobenzo[4,5]imidazo[1,2-c]quinazoline **2** and phenyl-5,5',6,6'-dihydrobenzo[4,4',5,5']imidazo[1.1',2-c,2'-c]quinazoline **3**.¹⁰ Characterization of **1–3** has been achieved by satisfactory elemental analyses, FT-IR, NMR

* Corresponding authors. Tel.: +91 542 6702480; fax: +91 542 2368174.

E-mail addresses: dspbhu@bhu.ac.in, dsprewa@yahoo.com (D.S. Pandey).



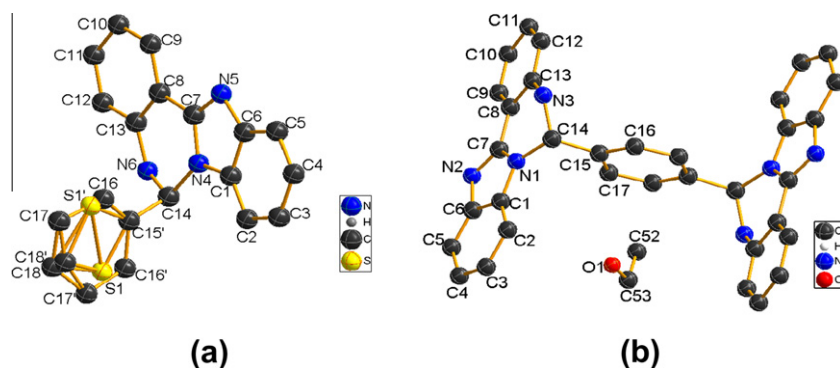
Scheme 1. One pot synthesis of probes 1–3.

(^1H and ^{13}C), HRMS and electronic absorption and emission studies. Structures of **1** and **3** have been determined by X-ray single crystal analyses. It is worth mentioning that **3** possesses two stereogenic centers therefore may exist in diastereomeric forms. However, both stereogenic centres are too far apart from each other for the existence of any diastereoselective relay during the synthesis. ^1H NMR spectral data of **1–3** along with their assignments have been gathered in Supplementary data (pp. S15). ^1H NMR spectra of **1** displayed singlets associated with $-\text{NH}$ and $-\text{CH}$ protons at δ 7.73 and 7.18 ppm (Fig. S1). Similarly, signals due to $-\text{NH}/-\text{CH}$ protons of **2** and **3** appeared at δ 7.69/7.13, **2** and 7.53/7.01 ppm **3** (Figs. S1–S3). It indicated C–N coupling through initially formed Schiff base (Scheme S2).

Diffraction quality crystals for **1** were obtained from methanolic solution at RT, while those for **3** by cooling the ethanolic reaction mixture. Selected crystallographic and refinement data for **1** and **3** are summarized in Table S1 (Supplementary data). Compound **1** crystallizes in monoclinic system with ' $P2_1/c$ ' space group, while **3** in triclinic system with ' $P-1$ ' group. Crystal structure of **1**

displayed a disordered thiophene ring which is very typical of 2-thienyl substituted compounds (Fig. 1a). An artificial lowering of the bond lengths with disordered atoms and high values of geometrical parameters have been observed by ignoring the disorder.

It is rather simple and can be a suitable example of negating effect for structural studies. The C(14)–N(6)/C(14)–N(4) bond lengths are almost equal (1.454/1.453 Å) and strongly suggest bonding of N(6) and N(4) to carbon C(14) through a single bond. It can be clearly seen that sulfur (S1/S1') lies perpendicular to N(4) N(6) nitrogen. The N(6)–H(6)···N(5) are involved in intermolecular hydrogen bonding interactions with N–H and N–N bond distances of 2.246 and 2.953 Å, respectively. The N–H–N angle between N(6)–H(6)–N(5) involved in hydrogen bonding interaction is 139.44°. Among these, the core created between thiophene sulfur (S1/S1') and quinazoline nitrogen (N6) may best be suited for interaction with cations. The asymmetric unit of **3** contains three symmetrical *trans*-oriented molecules, two half units of **3** and two ethanol molecules with the chemical formula moiety $\text{C}_{34}\text{H}_{24}\text{N}_6, 0.5(\text{C}_{34}\text{H}_{22}\text{N}_6), 2(\text{C}_2\text{H}_6\text{O})$ (see CIF; Fig. 1b). The ethanol

Figure 1. Crystal structures of **1** (a) and **3** (b) with atom numbering scheme (H atoms omitted for clarity).

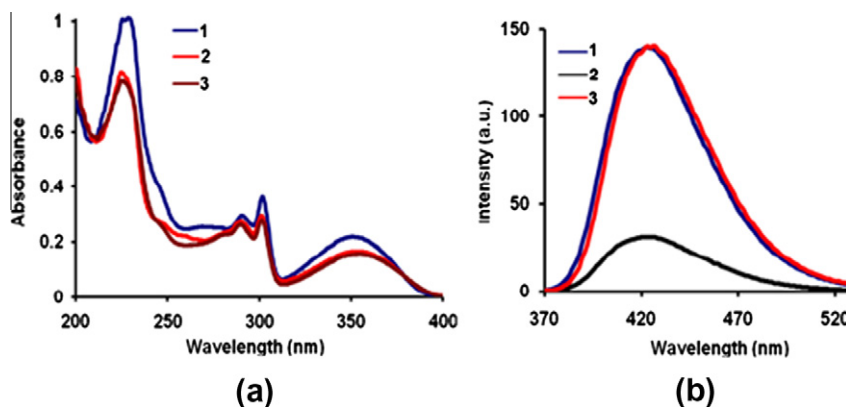


Figure 2. Absorption (a) and fluorescence [$\lambda_{\text{ex}} = 350$ nm, $\lambda_{\text{em}} = 423$ nm; PMT 400 V] (b) spectra of **1–3**, in H₂O/ EtOH (60: 40, pH \sim 7.2; c, 10 μ M) solution.

molecules are held with molecular units of **3** through intermolecular hydrogen bonding. The crystal structure strongly supported the formation of **3** with some disorder at N(7), N(8) and N(9) (see CIF). Compound **3** bears two identical stereogenic centers wherein one lies above and the other below the molecular plane.

The optical properties (absorption and emission) of **1–3** have been investigated in water/ethanol (60:40) using 10 μ M solution and the resulting data are summarized in Table S2. Electronic absorption spectrum of **1** exhibited bands at 291, 302 and 352 nm assignable to $\pi \rightarrow \pi^*$ and $n \rightarrow \pi^*$ intramolecular charge transfer (ICT) transitions (Fig. 2a).

Compounds **2** and **3** followed a similar pattern and exhibited bands at almost the same position [λ , 289, 301 and 355 nm, **2**; 291, 302 and 356 nm, **3**]. This observation is consistent with analogous structural features and the extent of conjugation in **1–3**. Further, to have an idea about influence of the solvent polarity, absorption and emission spectra of **1–3** (10 μ M) were acquired in various solvents (Table S3). In a polar solvent like DMSO the low energy band of **1** appeared at 359 nm (red shift). On the other hand, in benzene (non polar) it exhibited moderate blue shift, and in dichloromethane (semi-polar) a blue shift of \sim 5–6 nm (Fig. S6). The red and blue shifts in the position of absorption band may be ascribed to the extent of polarization of the probe in various solvents.¹¹ As expected, **2** and **3** followed an analogous pattern (Fig. S6).

Planar benzoannulated compounds fluoresce and find wide application as fluorescent probes.^{8,12} The compounds under investigation may also exhibit significant fluorescence. Upon excitation

at 350 nm, these strongly emit at 423 (**1**), 423 (**2**) and 426 nm (**3**). Resulting spectra are shown in Fig. 2b and data collected in Table S2. The emission band corresponding to **1** blue shifted in non polar solvents (Fig. S7) and exhibited a red shift of \sim 10–15 nm in protic polar solvents. On the other hand, emission spectra of **2** and **3** showed insignificant changes upon varying the solvent polarity (Fig. S7). The quantum yields for **1–3** (Φ_f , pyrene) have been determined to be 0.76, 0.20 and 0.62.^{13b} Based on the absorption and emission spectral behaviour, **1** has been chosen as the key probe for further studies.

To understand the affinity of **1–3** towards various metal ions both absorption and emission spectral studies have been performed in the presence of cations like Na⁺, K⁺, Ca²⁺, Mg²⁺, Mn²⁺, Co²⁺, Ni²⁺, Cu²⁺, Zn²⁺, Ag⁺, Cd²⁺, Pb²⁺ and Hg²⁺ (nitrate salts) in water/ethanol (60: 40, v/v; c, 10 mM). Upon addition of an excess of tested metal ions (20.0 equiv; c, 10 mM) the absorption spectra of **1–3** exhibited insignificant changes except for Hg²⁺ (Fig. 3 and S12). The band centred at 352 nm in the spectrum of **1** exhibited a bathochromic shift upon addition of an excess of Hg²⁺ and appeared at \sim 374 nm, while high energy band showed a marginal red shift ($\Delta\lambda$, \sim 4 nm). In an analogous manner, lower energy bands of **2** and **3** displayed relatively small bathochromic shifts (\sim 360 nm, **2**; \sim 365 nm, **3**; Fig. S12).

Metal ion interaction studies for **1–3** were followed by emission spectral studies (λ_{ex} , 350 nm) in the presence of tested metal ions (20.0 equiv, Fig. 3b and S10). The emission band present at 423 nm in the spectrum of **1** quenches upon addition of Hg²⁺ (\sim 83%), while other metal ions were ineffective in this regard. Similarly, **2** and **3**

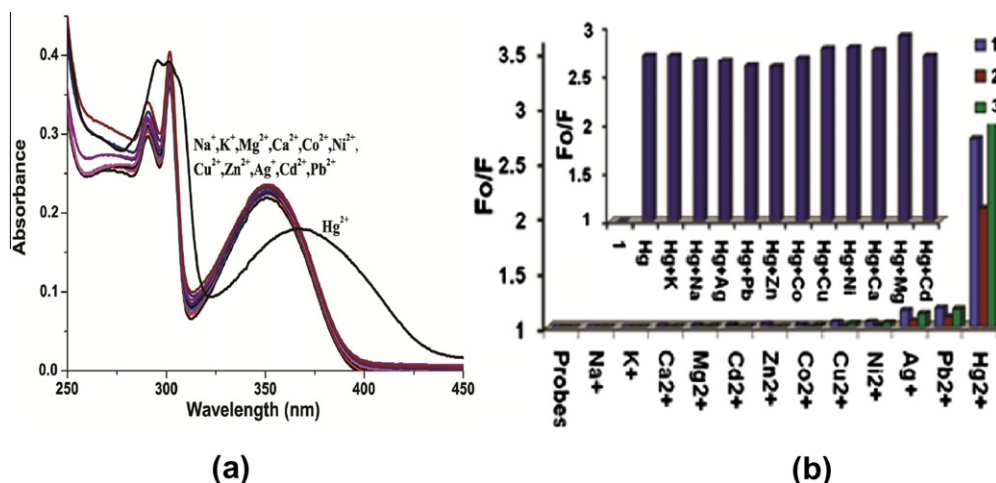


Figure 3. (a) Absorption spectra of **1** (10 μ M) in the presence of metal nitrates (20 equiv, c, 10 mM). (b) Bar diagram showing relative fluorescence intensity for **1–3** (c, 10 μ M) in the presence of various metal ions. Inset showing the interference study for **1**+Hg²⁺ with various metal ions.

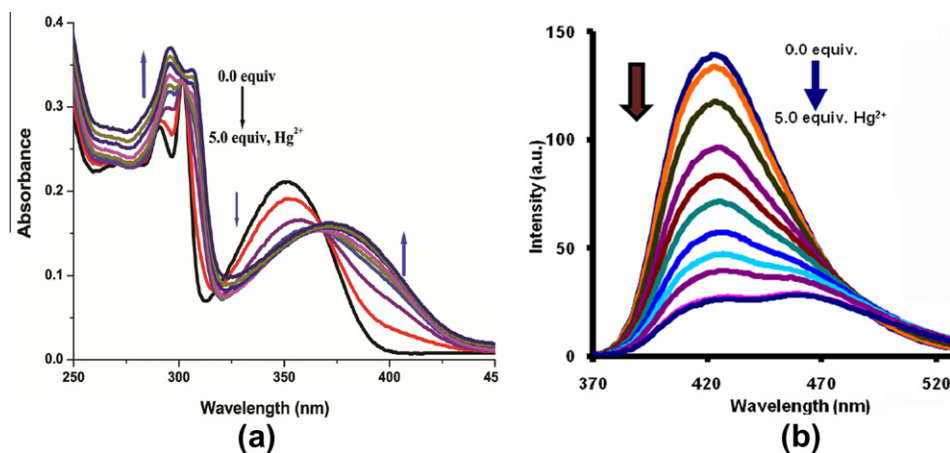


Figure 4. (a) Absorption and (b) emission titration spectra of **1** (c, 10 μM) in the presence of various equiv of Hg^{2+} .

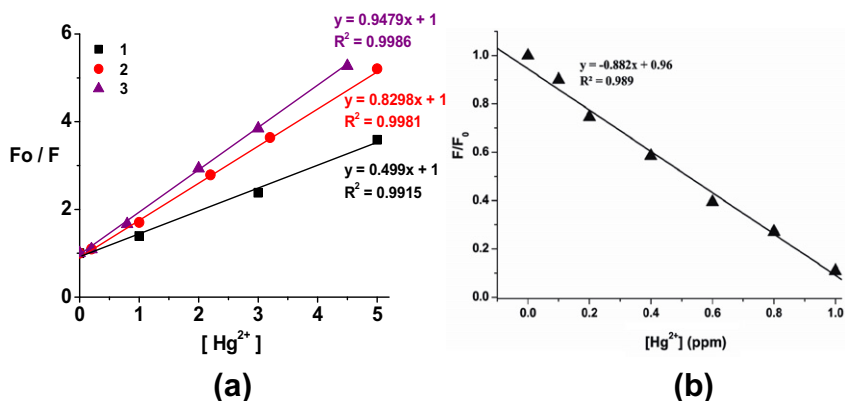


Figure 5. (a) Stern-Volmer plots for **1–3** for estimation of quenching constants in the presence of Hg^{2+} . (b) Linear fluorescence intensity (F/F_0 , $R^2 = 0.99$) of **1** (1.0 μM) upon addition of Hg^{2+} (0–1.0 μM).

exhibited fluorescence quenching of ~ 77 and 86% in the presence of Hg^{2+} (Fig. 3b and S10). To follow selectivity of **1** towards Hg^{2+} , interference studies were performed under analogous conditions by the addition of an excess of (20 equiv) metal ions including Cu^{2+} , Cd^{2+} , Pb^{2+} and Ag^+ to a solution of **1** containing Hg^{2+} . Notably, fluorescence intensity of the probable **1**+ Hg^{2+} complex (Fig. 3b, inset) remains more or less the same in the presence of other metal ions, suggesting higher affinity and selectivity of **1** for Hg^{2+} .

The biological applications of probes require sensing in a wide pH range. The effect of pH on absorption and fluorescence response of **1** towards Hg^{2+} implies that the probe operates well in the pH range of 6.0–7.4 (c, 5 μM ; Fig. S9). It was observed that the actual species exists at pH ~ 7.2 and an increase (pH ~ 8.4 ; ϵ , $0.0977 \text{ M}^{-1}\text{cm}^{-1}$) or decrease of the pH (pH ~ 6.0 ; ϵ , $0.1068 \text{ M}^{-1}\text{cm}^{-1}$) diminishes optical density of **1** at 351 nm (Fig. S9a). In contrast fluorescence intensity increases at higher pH (pH ~ 8.4) and is quenched at lower pH (pH ~ 6.0) in **1** (Fig. S9b).

To get deep insight into sensitivity and binding of **1** with Hg^{2+} , absorption titrations were carried out by sequential addition of $\text{Hg}(\text{NO}_3)_2$ (c, 10 mM; 0.0–5.0 equiv) to a solution of **1** (c, 10 μM) in ethanol/water (60:40, v/v). Upon addition of Hg^{2+} molar extinction coefficient of the low energy band (λ , $\sim 352 \text{ nm}$; ϵ , $21,100 \text{ cm}^{-1}\text{M}^{-1}$) decreases to $\sim 5,000 \text{ cm}^{-1}\text{M}^{-1}$, concomitantly a new band appeared at λ , $\sim 374 \text{ nm}$ (Fig. 4a). The appearance of an isosbestic point at $\sim 369 \text{ nm}$ suggested the presence of more than two species in the medium. Similarly, bands due to high energy $\pi \rightarrow \pi^*$ transitions rationalized and red shifted to appear at 297 and 306 nm. The UV–vis behaviour of **2** and **3** was almost similar to **1** (Fig. S11).

The selectivity of **1–3** for Hg^{2+} was further followed by fluorescence titration studies under similar conditions. Addition of Hg^{2+} (0.0–5.0 equiv) to a solution of **1** leads to a gradual decrease in fluorescence intensity of the band centred at λ , $\sim 423 \text{ nm}$ (83% , ~ 6.0 -fold, Figs. 4b and 6, inset) and decrease in the quantum yield ($\Delta\Phi_f = 0.65$). Analogous fluorescence quenching has been observed for **2** (λ , 423 nm) and **3** (λ , 426 nm) also, in the presence of Hg^{2+} (Table S2, Fig. S12). Observed bathochromic shifts of both the low and high energy bands and a decrease in relative fluorescence intensity may be attributed to the CT process from the receptor site to quinazoline ring and enhanced photoinduced electron transfer process (PET).¹⁴ To assess the sensitivity, varying concentrations of Hg^{2+} (0.1–1.0 μM) were added to solution containing 1.0 μM of **1** (Fig. 5b). A plot between fluorescence intensity vs. concentration of Hg^{2+} (0.1–1.0 μM) exhibited a linear relationship ($R^2 = 0.99$), suggesting the limit of detection (LOD) of $2.0 \times 10^{-7} \text{ M}$ and that **1** is potentially useful for the detection of Hg^{2+} .

Job's plot analysis revealed that **1** and **2** interact with Hg^{2+} in 1:1, while **3** in 1:2 (probe/metal) stoichiometries (Fig. S13). Further, the binding affinity of **1–3** for Hg^{2+} was estimated from Benesi-Hildebrand plots.¹⁵ The association constants (K_a) for **1–3** based on non-linear fitting of emission titration data using 1:1 and 1:2 binding model have been found to be $1.34 \pm 0.004 \times 10^4 \text{ M}^{-1}$ (**1**), $3.40 \pm 0.03 \times 10^3 \text{ M}^{-1}$ (**2**) and $3.78 \pm 0.03 \times 10^6 \text{ M}^{-2}$ (**3**) (Fig. S14).¹⁵ Quenching efficiency of **1–3** has been estimated quantitatively from Stern-Volmer plots (Fig. 5a) and found to be $K_{sv} = 9479$ (**1**); 8298 (**2**) and 9980 M^{-1} (**3**). Binding constant for **3** is much higher relative to **1** and **2** which may be attributed to

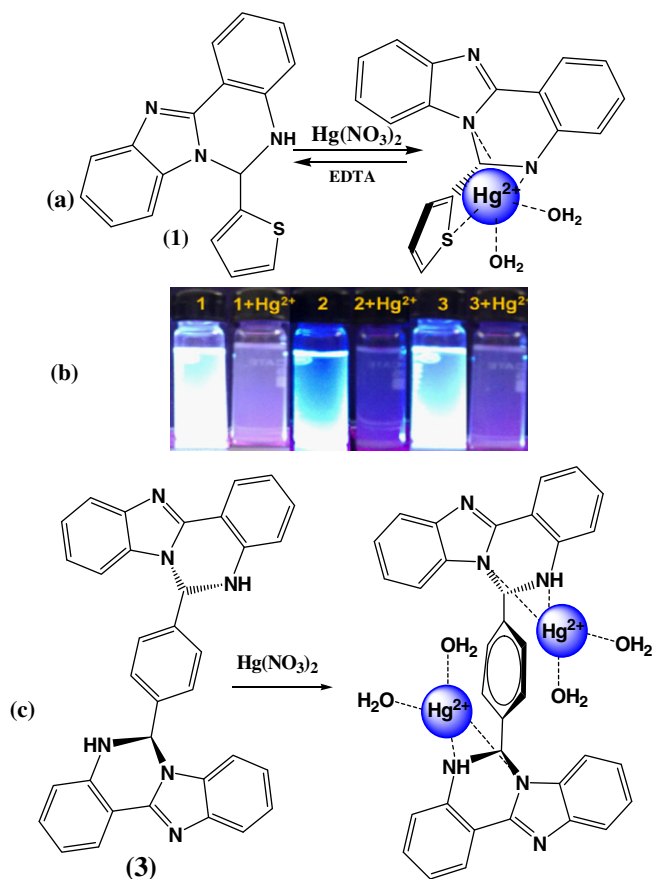


Figure 6. (a) Reversible binding mode of **1** with Hg^{2+} in the presence of excess EDTA. (b) Fluorescence intensity change in **1–3** in the presence of Hg^{2+} . (c) Plausible binding mode of **3** with Hg^{2+} .

1:2 (**3**: Hg^{2+}) stoichiometry. Overall data suggested that probes **1–3** act as sensitive and selective chemosensors for Hg^{2+} through 'on-off' signalling.

The interaction of **1** with Hg^{2+} was also followed by the addition of large amounts of a strong chelating agent like EDTA to a solution of **1**+ Hg^{2+} , which resulted in the regeneration of the band due to **1** both in the absorption and emission spectra (Fig. S15). It suggested reversible interaction between **1** and Hg^{2+} (Fig. 6a). One may think that the process may involve liberation of Hg^{2+} from **1**+ Hg^{2+} and its interaction with EDTA to form a more stable EDTA- Hg^{2+} complex. To ascertain this, ~20.0 equiv of Hg^{2+} was added to a solution of **1** leading to fluorescence quenching to a large extent. Further, addition of an excess of EDTA (200.0 equiv) to this solution led to regeneration of emission band. In turn, addition of EDTA (100.0 equiv) to a solution of **1** led to insignificant changes in the position of emission band, whereas addition of 40.0 equiv of Hg^{2+} led to fluorescence quenching to some extent (Fig. S15c). The above observations clearly indicated that EDTA itself does not interfere with **1**, but accepts back the Hg^{2+} from **1**+ Hg^{2+} complex.

Initially, **1** containing a suitable chelating site represented by S and N is expected to interact with Hg^{2+} more effectively over other cations. Expectedly, it exhibited significant change in the absorption and emission spectra only in the presence of Hg^{2+} . To further ascertain whether sulphur atom of the quinazoline core is responsible for Hg^{2+} -induced 'turn-off' signalling, some other quinazoline derivatives (**2** and **3**) having 6-substituted hetero-rings with hetero atoms at different positions were synthesized. Notably, **3** also selectively binds with Hg^{2+} in analogous manner through both interacting sites and displayed fluorescence quenching (Fig. 6).

The results strongly suggested that quinazoline core in **1–3** leads to Hg^{2+} -selective 'turn-off' signalling, not hetero-rings attached at 6-position, though the presence of a hetero atom at suitable chelation site may increase the sensitivity and stability of the ensuing product. Based on the present study it may be concluded that more quinazolines possessing appropriate 6-hetero rings that can be designed and prepared following current protocol that can serve as highly Hg^{2+} -selective 'on-off' probes with increased/decreased sensitivity. The fluorescence intensity of **1–3** is very high so the fluorescence studies have been performed at PMT 400 V.

To establish the interaction site of **1** with Hg^{2+} , ^1H NMR titration experiment was performed in $\text{DMSO}-d_6$ (Fig. S16). Upon addition of $\text{Hg}(\text{ClO}_4)_2$ (0.5 equiv) to a solution of **1**, the aromatic ring protons exhibited deshielding. The H1 proton due to NH ionophore (br. s, δ 7.73 ppm) shifted downfield to appear at δ 8.17 ppm (Fig. S1). Signals due to H3, H10 and H11, H12 protons merged together and appeared as a multiplet at δ 7.43–7.38 ppm. However, merged resonances due to H2 and H4 separated after addition of Hg^{2+} and appeared at δ 7.68 and 7.62 ppm, respectively. With an increase in the concentration of Hg^{2+} (1.0–2.0 equiv), signals due to $-\text{NH}$ and H2/H4 protons exhibited a downfield shift and appeared at δ 8.54 ($\Delta\delta$, 0.81) and δ 7.86 ppm ($\Delta\delta$, 0.39), respectively. Similarly, signals due to H3, H11 and H12 protons merged and resonated in the range of δ 7.48–7.54, while H5 at δ 7.32 ppm ($\Delta\delta$ = 0.12). The H5 ($-\text{CH}$) exhibited a smaller downfield shift relative to $-\text{NH}$ (H1) proton. Downfield shift observed for all the protons clearly indicated interaction of **1** with Hg^{2+} ion. ^1H NMR titration results suggested the interaction of Hg^{2+} with **1** probably, through both the quinazoline N and thiophene 'S' donor sites. As **1** offers three interaction sites, the most probable geometry about Hg^{2+} may be a distorted trigonal bipyramidal¹⁶ (Fig. S20), which has further been supported by mass spectral studies (*vide supra*). Further, to investigate the involvement of 'N' atom of benzimidazole unit besides $-\text{NH}$ with Hg^{2+} , ^1H NMR titration experiments were performed using symmetrical probe **3**, which lacks thiophene/ pyridine rings (Fig. S17). The appearance of only a singlet at δ 8.31 ppm ($-\text{NH}$) after complete binding with Hg^{2+} (see Supplementary data, pp. S24–25) suggested the involvement of quinazoline ($-\text{NH}$) and one benzimidazole nitrogen of both the stereogenic sites (Fig. 6c and S20).

Analysis of the HRMS data further supported the formation of probes **1–3** and the species arising from interaction between **1** and Hg^{2+} . The molecular ion peak $[\text{M}+1]^+$ for **1–3** (100%) appeared at m/z 304.0906 (calc. 304.0830), 299.1294 (calc. 299.1218) and 517.2141 (calc. 517.2062), respectively (Fig. S18). To provide further support to 1:1 stoichiometry between **1** and Hg^{2+} , HRMS spectrum of a $[\text{1}+\text{Hg}(\text{H}_2\text{O})_2](\text{NO}_3)_2$ was acquired. It displayed a peak assignable to $[\text{M}]^+$ at m/z 541.0869 (541.0748), corresponding to $[\text{1}+\text{Hg}(\text{H}_2\text{O})_2]^{2+}$ (Fig. S18).¹⁷ In addition, to have an idea about the possibility of $-\text{NH}$ deprotonation upon interaction with Hg^{2+} ions, (Figs. S16 and S20) FAB-MS spectra of the compound obtained by treatment of $\text{Hg}(\text{NO}_3)_2$ with probe **1**, was acquired. The spectrum exhibited a peak corresponding to $[\text{M}]^+$ of 1:1 complex $[\text{1}+\text{Hg}(\text{H}_2\text{O})_2](\text{NO}_3)_2$ at m/z 665 (665) along with other peaks (Fig. S19). The presence of both nitrates as counter anions strongly supported that deprotonation of $-\text{NH}$ proton is not taking place during interaction with Hg^{2+} ions.

Crystal structure of **1** shows that 'S' is disposed away from $-\text{NH}$, that can structurally reorient upon interaction with Hg^{2+} to facilitate the chelation process.^{18a} From crystal structures of **1** and **3** (Fig. 1) it is obvious that 6-substituted hetero ring may undergo conformational changes in the presence of Hg^{2+} ion (Fig. 1). The observed fluorescence quenching may be attributed to the formation of a mercury complex^{18b–d} It may also arise due to proximity of the metal with unpaired electrons of the ligand which may lead to spin-orbit coupling and enhanced intersystem crossing.^{18e} The

'turn-off' signalling with LOD 2.0×10^{-7} M for Hg^{2+} suggested the possible applications of quinazolines for Hg^{2+} detection. It is worth mentioning that though **1–3** detect Hg^{2+} through 'turn-off' signalling, their selectivity for this cation is extremely high. Overall, this approach provides a straightforward pathway to develop quinazoline receptors for Hg^{2+} sensing in aqueous media.

In this work we have designed and synthesized some new quinazolines **1–3** in reasonably good yield. Structures of **1** and **3** have been determined crystallographically. The compounds under study exhibit strong fluorescence at RT. The Hg^{2+} detection has been demonstrated by absorption, fluorescence, ^1H NMR, HRMS and FAB-MS spectral studies. Fluorescence intensity of **1–3** quenches selectively in the presence of Hg^{2+} in 1:1 stoichiometry with **1** and **2**, while 1:2 (probe/metal) with **3**. The interaction site of probes has been suggested by ^1H NMR titration studies. These three probes **1–3** possess different hetero-aryl rings at 6-position; nevertheless displayed a 'turn-off' switching behaviour selectively for Hg^{2+} under aqueous conditions.

Acknowledgements

Thanks are due to the Department of Science and Technology (DST), New Delhi, India for providing financial assistance through the Scheme SR/S1/IC-15/2006. One of the authors (RP) is grateful to the Council of Scientific and Industrial Research (CSIR), New Delhi, India for providing financial assistance through Senior Research Fellowship (9/13(288)/2010-EMR-I).

Supplementary data

Instrumental details, ^1H and ^{13}C NMR spectra, experimental details of **1–3**, scheme for the preparation of **1–4**, ^1H NMR description for **1–3**, absorption and fluorescence data, B-H plots for binding constants, binding modes of **1** and **3** with Hg^{2+} , Mass spectra, crystallographic data of **1** and **3** in CIF format [CCDC deposition Nos. 792047 (**1**) and 792048 (**3**)].

Supplementary data associated with this article can be found, in the online version, at <http://dx.doi.org/10.1016/j.tetlet.2012.04.128>.

References and notes

- (a) Nolan, E. M.; Lippard, S. J. *Chem. Rev.* **2008**, *108*, 3443–3480; (b) Fabbrizzi, L.; Poggi, A. *Chem. Soc. Rev.* **1995**, 197–202; Martínez-Máñez, R.; Sancenón, F. *Chem. Rev.* **2003**, *103*, 4419; (c) Kim, H. N.; Lee, M. H.; Kim, H. J.; Kim, J. S.; Yoon, J. *Chem. Soc. Rev.* **2008**, *37*, 1465–1472; (d) Huang, W.; Song, C.; He, C.; Lv, G.; Hu, X.; Zhu, X.; Duan, C. *Inorg. Chem.* **2009**, *48*, 5061; (e) Li, H.; Zhai, J.; Sun, X. *Analyst* **2011**, *136*, 2040–2043; (f) Coskun, A.; Yilmaz, M. D.; Akkaya, E. U. *Org. Lett.* **2007**, *9*, 607–609; (g) Ho, M.-L.; Chen, K.-Y.; Lee, G.-H.; Chen, Y.-C.; Wang, C.-C.; Lee, J.-F.; Chung, W.-C.; Chou, P. T. *Inorg. Chem.* **2009**, *48*, 10304–10311.
- (a) Valeur, B.; Leray, I. *Coord. Chem. Rev.* **2000**, *205*, 3–40; (b) Amendola, V.; Fabbrizzi, L.; Licchelli, M.; Mangano, C.; Pallavicini, P.; Parodi, L.; Poggi, A. *Coord. Chem. Rev.* **1999**, *190–192*, 649–669; (c) Nikolaev, V. O.; Gambaryan, S.; Lohse, M. J. *Nature Methods* **2006**, *3*, 23–25; (d) Zhang, J.; Campbell, R. E.; Ting, A. Y.; Tisen, R. Y. *Nat. Rev. Mol. Cell Biol.* **2002**, *3*, 906–918; (e) *Chemosensors for Ion and Molecule Recognition*; Desvergne, J. P., Czarnik, A. W., Eds.; Kluwer Academic Publishers: Dordrecht, The Netherlands, 1997; (f) Huang, S.; Clark, R. J.; Zhu, L. *Org. Lett.* **2007**, *9*, 4999–5002; (g) Ma, D.-L.; Chan, D. S.-H.; Man, B. Y.-W.; Leung, C.-H. *Chem-An Asian J.* **2011**, *6*, 986–1003.
- (a) Tchounwou, P. B.; Ayensu, W. K.; Ninashvili, N.; Sutton, D. *Environ. Toxicol.* **2003**, *18*, 149–175; (b) Farina, M.; Soares, F. A.; Feoli, A.; Roehring, C.; Brusque, A. M.; Rotta, L.; Perry, M. L.; Souza, D. O.; Rocha, J. B. T. *Nutrition* **2003**, *19*, 531–535.
- (a) Ko, S.-K.; Yang, Y.-K.; Tae, J.; Shin, I. *J. Am. Chem. Soc.* **2006**, *128*, 14150–14155; (b) Yang, H.; Zhou, Z.; Huang, K.; Yu, M.; Li, F.; Yi, T.; Huang, C. *Org. Lett.* **2007**, *9*, 4729–4732; (c) Kim, J. S.; Noh, K. H.; Lee, S. H.; Kim, S. K.; Kim, S. K.; Yoon, J. *J. Org. Chem.* **2003**, *68*, 597–600; (d) Chen, Q.-Y.; Chen, C.-F. *Tetrahedron Lett.* **2005**, *46*, 165–168; (e) Moon, S. Y.; Cha, N. R.; Kim, Y. H.; Chang, S.-K. *J. Org. Chem.* **2004**, *69*, 181–183.
- (a) Zhang, J. F.; Kim, J. S. *Anal. Sci.* **2009**, *25*, 1271–1281; (b) Xie, A. J.; Zheng, Y.; Ying, J. Y. *Chem. Commun.* **2010**, *46*, 961–963; (c) Tsukamoto, K.; Shinohara, Y.; Iwasaki, S.; Maeda, H. *Chem. Commun.* **2011**, *47*, 5073–5075; (d) Liu, X.; Shu, X.; Zhou, X.; Zhang, X.; Zhu, J. *J. Phys. Chem. A* **2010**, *114*, 13370–13375; (e) Shiraiishi, Y.; Sumiya, S.; Hirai, T. *Org. Biomol. Chem.* **2010**, *8*, 1310–1314.
- (a) Yu, Y.; Lin, L.-R.; Yang, K.-B.; Zhong, X.; Huang, R.-B.; Zheng, L.-S. *Talanta* **2006**, *69*, 103–106; (b) de Silva, A. P.; Fox, D. P.; Huxley, A. J. M.; Moody, T. S. *Coord. Chem. Rev.* **2000**, *205*, 41–57; (c) Bag, B.; Bharadwaj, P. K. *Inorg. Chem.* **2004**, *43*, 4626–4630; (d) Suresh, M.; Jose, D. A.; Das, A. *Org. Lett.* **2007**, *9*, 441–444; (e) Ghosh, A.; Ganguly, B.; Das, A. *Inorg. Chem.* **2007**, *46*, 9912–9918.
- (a) Morguntsova, S. A.; Belenichev, I. F.; Abramov, A. V. *Dosyagennyya Biologii ta Meditsini* **2009**, *2*, 67–70; (b) Ismail, M. A. H.; Barker, S.; El Ella, D. A. A.; Abouzid, K. A. M.; Toubar, R. A.; Todd, M. H. *J. Med. Chem.* **2006**, *49*, 1526–1535; (c) Galandová, J.; Ovádeková, R.; Ferancová, A.; Labuda, J. *Anal Bioanal Chem* **2009**, *394*, 855–861; (d) Gellibert, F.; Fouchet, M.-H.; Nguyen, V.-L.; Wang, R.; Krysa, G.; de Gouville, A.-C.; Huet, S.; Dodic, N. *Bioorg. Med. Chem. Lett.* **2009**, *19*, 2277–2281.
- (a) Saha, U. C.; Chattopadhyay, B.; Dhara, K.; Mandal, S. K.; Sarkar, S.; Khuda-Bukhsh, A. R.; Mukherjee, M.; Helliwell, M.; Chattopadhyay, P. *Inorg. Chem.* **2011**, *50*, 1213–1219; (b) Luoa, H.-Y.; Zhang, X.-B.; Hea, C.-L.; Shen, G.-L.; Yu, R.-Q. *Spectrochim. Acta (A)* **2008**, *70*, 337–342; (c) Chinigo, G. M.; Paige, M.; Grindrod, S.; Hamel, E.; Dakshanamurthy, S.; Chruszcz, M.; Minor, W.; Brown, M. L. *J. Med. Chem.* **2008**, *51*, 4620–4631.
- (a) Booysen, I.; Gerber, A. I. A.; Mayer, P. J. *Coord. Chem.* **2008**, *61*, 1525–1531; (b) Chhonker, Y. S.; Veenus, B.; Hasim, S.; Kaushik, R. N.; Kumar, D.; Kumar, P. *E-J. Chem.* **2009**, *6*, S342.
- (a) Rohini, R.; Shanker, K.; Reddy, P. M.; Ho, Y.-P.; Ravinder, V. *Eur. J. Med. Chem.* **2009**, *44*, 3330–3339; (b) Lyakhova, E. A.; Gusyeva, Y. A.; Nekhoroshkova, J. V.; Shafran, L. M.; Lyakhov, S. A. *Eur. J. Med. Chem.* **2009**, *44*, 3305–3312.
- Misra, A.; Shahid, M. J. *Phys. Chem. C* **2010**, *114*, 16726–16739.
- (a) Hirano, K.; Oderaotoshi, Y.; Minataka, S.; Unique, K. M. *Chem. Lett.* **2001**, 1262–1263; (b) Vivas-Mejía, P.; Rodríguez-Cabán, J. L.; Díaz-Velázquez, M.; Hernández-Pérez, M. G.; Cox, O.; Gonzalez, F. A. *Mol. Cell. Biochem.* **1997**, *177*, 69–77.
- (a) Shirdel, J.; Penzkofer, A.; Procházka, R.; Shen, Z.; Strauss, J.; Daub, J. *Chem. Phys.* **2007**, *331*, 427–437; (b) Yslas, E. I.; Rivarola, V.; Durantini, E. N. *Bioorg. Med. Chem.* **2005**, *13*, 39–46; (c) Lin, P. *Chem. Rev.* **2004**, *104*, 1687–1716; (d) Prabhakar, M.; Zacharias, P. S.; Das, S. K. *Inorg. Chem.* **2005**, *44*, 2585–2587.
- (a) Goodall, W.; Williams, J. A. G. *Chem. Commun.* **2001**, 2514–2515; (b) Goswami, S.; Sen, D.; Das, N. K.; Hazra, G. *Tetrahedron Letters* **2010**, *51*, 5563–5566; (c) Wang, J.; Qian, X.; Cui, J. *J. Org. Chem.* **2006**, *71*, 4308–4311.
- (a) Connors, K. A. *Binding Constants*; Wiley: New York, 1987; (b) Benesi, H. A.; Hildebrand, J. H. *J. Am. Chem. Soc.* **1949**, *71*, 2703; (c) Mashraqui, S. H.; Khan, T.; Sundaram, S.; Betkar, R.; Chandiramani, M. *Tetrahedron Lett.* **2007**, *48*, 8487–8490.
- Zhou, H.-P.; Gan, X.-P.; Li, X.-L.; Liu, Z.-D.; Geng, W.-Q.; Zhou, F.-X.; Ke, W.-Z.; Wang, P.; Kong, L.; Hao, F.-Y.; Wu, J.-Y.; Tian, Y.-P. *Cryst Growth & Des.* **2010**, *10*, 1767–1776.
- (a) Wu, Z.; Zhang, Y.; Ma, J. S.; Yang, G. *Inorg. Chem.* **2006**, *45*, 3140–3142; (b) Fukushima, K.; Iwahashi, H. *Chem. Commun.* **2000**, 895–896.
- (a) Melnick, J. G.; Yurkerwich, K.; Parkin, G. *Inorg. Chem.* **2009**, *48*, 6763–6772; (b) Wang, F.; Schwabacher, A. W. *J. Org. Chem.* **1999**, *64*, 8922–8928; (c) Moon, S.-Y.; Youn, N. J.; Park, S. M.; Chang, S.-K. *J. Org. Chem.* **2005**, *70*, 2394–2397; (d) Rurack, K. *Spectrochim. Acta, A* **2001**, *57*, 2161–2195; (e) *Probe Design and Chemical Sensing In Topics in Fluorescence Spectroscopy*; Lakowicz, J. R., Ed.; Kluwer: Hingham, 1994; Vol. 4, p 56.